1521-0111/84/5/774–786$25.00
MOLECULAR PHARMACOLOGY

http://dx.doi.org/10.1124/mol.113.086298
Mol Pharmacol 84:774–786, November 2013

Acetaminophen Modulates P-Glycoprotein Functional Expression at the Blood-Brain Barrier by a Constitutive Androstane Receptor–Dependent Mechanism

Lauren M. Slosky, Brandon J. Thompson, Lucy Sanchez-Covarrubias, Yifeng Zhang, Mei-Li Laracuente, Todd W. Vanderah, Patrick T. Ronaldson, and Thomas P. Davis

Department of Medical Pharmacology, University of Arizona College of Medicine, Tucson, Arizona

Received March 13, 2013; accepted September 9, 2013

ABSTRACT

Effective pharmacologic treatment of pain with opioids requires that these drugs attain efficacious concentrations in the central nervous system (CNS). A primary determinant of CNS drug permeation is P-glycoprotein (P-gp), an endogenous blood-brain barrier (BBB) efflux transporter that is involved in brain-to-blood transport of opioid analgesics (i.e., morphine). Recently, the nuclear receptor constitutive androstane receptor (CAR) has been identified as a regulator of P-gp functional expression at the BBB. This is critical to pharmacotherapy of pain/inflammation, as patients are often administered acetaminophen (APAP), a CAR-activating ligand, in conjunction with an opioid. Our objective was to investigate, in vivo, the role of CAR in regulation of P-gp at the BBB. Following APAP treatment, P-gp protein expression was increased up to 1.4–1.6-fold in a concentration-dependent manner. Additionally, APAP increased P-gp transport of BODIPY-verapamil in freshly isolated rat brain capillaries. This APAP-induced increase in P-gp expression and activity was attenuated in the presence of CAR pathway inhibitor okadaic acid or transcriptional inhibitor actinomycin D, suggesting P-gp regulation is CAR-dependent. Furthermore, morphine brain accumulation was enhanced by P-gp inhibitors in APAP-treated animals, suggesting P-gp–mediated transport. A warm-water (50°C) tail-flick assay revealed a significant decrease in morphine analgesia in animals treated with morphine 3 or 6 hours after APAP treatment, as compared with animals treated concurrently. Taken together, our data imply that inclusion of APAP in a pain treatment regimen activates CAR at the BBB and increases P-gp functional expression, a clinically significant drug-drug interaction that modulates opioid analgesic efficacy.

Introduction

Pain affects over 116 million people in the United States and costs ~$635 billion in medical treatments and lost productivity (Institute of Medicine, 2011; http://www.iom.edu/relievingpain). Pain is a dominant symptom associated with acute and chronic inflammatory conditions. Pharmacotherapy of pain often involves opioids, which are the most effective and the most widely used analgesic drugs. Opioids provide analgesia by binding to opioid receptors (i.e., μ, κ, δ) on peripheral nerves; however, fully efficacious analgesia requires that these drugs access central nervous system (CNS) opioid receptors (Hamabe et al., 2007; Labuz et al., 2007). Despite their analgesic efficacy, opioids are associated with multiple unwanted effects. They can cause euphoria that, in part, accounts for their abuse potential. Additionally, opioid pharmacotherapy can lead to respiratory depression, constipation, nausea, vomiting, and rapid development of tolerance (Ronaldson and Davis, 2011, 2013). These adverse effects limit the opioid dose that can be administered and the level of analgesia that can be attained. Therefore, it is critical that brain opioid concentrations be maintained precisely to ensure effective pain management and to limit adverse drug reactions.

Brain permeation of opioids is limited by the blood-brain barrier (BBB), a physical and biochemical barrier composed of microvascular endothelial cells surrounded by pericytes and astrocytes. BBB endothelial cells are joined by tight junctions/protein complexes, that impart a transendothelial resistance of 1500–2000 $\Omega \cdot cm^2$, thereby restricting drug permeability (Butt et al., 1990). The BBB also expresses efflux transporters, such as P-glycoprotein (P-gp), that greatly impair the ability of drugs to attain efficacious CNS concentrations. A member of the ATP-binding cassette superfamily of transporters, P-gp is a 170-kDa integral membrane protein that is encoded by the multidrug resistance (MDR) gene (Gottesman et al., 1995). Two isoforms of the MDR gene, designated MDR1 and MDR2, have been cloned and sequenced in humans (Chen et al., 1986; Roninson et al., 1986). In rodents, P-gp is encoded by three genes designated mdr1a, mdr1b, and mdr2. While MDR2/

This work was supported by the National Institutes of Health National Institute on Drug Abuse [Grant R01DA11271]; the American Association of Pharmaceutical Scientists' New Investigator Grant in Pharmacokinetics, Pharmacodynamics, and Drug Metabolism; and a University of Arizona Faculty Seed Grant.
dx.doi.org/10.1124/mol.113.086298.

ABBREVIATIONS: Act D, actinomycin D; ANOVA, analysis of variance; APAP, acetaminophen; BBB, blood-brain barrier; CAR, constitutive androstane receptor; CNS, central nervous system; CsA, cyclosporine A; DMSO, dimethyl sulfoxide; hCAR, human CAR; MDR, multidrug resistance; Mrp1, multidrug resistance-associated protein 1; OA, okadaic acid; PB, phenobarbital; P-gp, P-glycoprotein; PP2A, protein phosphatase 2A; PSC 833, 6-[(2*S*,4*R*,6*E*)-4-methyl-2-(methylamino)-3-oxo-6-octenoic acid]-7-L-valine-cyclosporin A.

mdr2 is primarily a hepatic transporter of phosphotidylcholine (Ueda et al., 1987), MDR1/mdr1a/mdr1b are expressed at multiple tissue barrier sites, including the BBB, and are involved in drug transport (Ueda et al., 1987; Gottesman et al., 1995). Since its discovery, many opioids and associated metabolites have been identified as P-gp substrates, including morphine (Letrent et al., 1998; Dagenais et al., 2004; Seelbach et al., 2007), morphine-6-glucuronide (Lotsch et al., 2002), and methadone (Bauer et al., 2006). P-gp is also involved in brain-to-blood transport of opioid analgesic peptides such as met-enkephalin and [D-penicillamine2,5]enkephalin (Dagenais et al., 2001; Kastin et al., 2002; Ronaldson et al., 2011).

Nuclear receptors, such as the constitutive androstane receptor (CAR), are ligand-activated transcription factors that are involved in P-gp regulation in several tissues, including brain microvasculature (Bauer et al., 2004, 2006; Wang et al., 2010; Chan et al., 2011). For example, CAR activation with the known activating ligand phenobarbital (PB) increased P-gp expression in isolated rat brain capillaries (Wang et al., 2010). This same study showed that PB treatment increased luminal accumulation of fluorescently labeled cyclosporine A (CsA), a known P-gp substrate, suggesting enhancement in P-gp transport (Wang et al., 2010). Although the presence of CAR at the rodent BBB is well established, its expression at the human BBB has been debated. While Dauchy and colleagues (2008) could not detect human CAR (hCAR) mRNA in isolated brain microvessels from epileptic or glioma patients, studies using an immortalized human brain microvessel endothelial cell line (hCMEC/D3) and human brain-derived microvascular endothelial cells reported expression of both hCAR mRNA and protein (Chan et al., 2011). Additionally, Chan and colleagues (2011) found that hCAR activation by 6-(4-chlorophenyl)-imidazo[2,1-b]thiazole-5-carbaldehyde increased P-gp expression, providing evidence for P-gp regulation at the human BBB. Such observations may have profound implications for pain management regimens. For example, acetaminophen (APAP), a known CAR activator (Zhang et al., 2002), is often administered in conjunction with morphine, a P-gp substrate, for treatment of postoperative pain (Remy et al., 2005). While CAR activation can increase P-gp functional expression at the BBB, the role of this mechanism in the context of pain pharmacotherapy has not been thoroughly examined.

In the present study, we investigated, in vivo, effects of a single APAP dose on P-gp functional expression at the BBB. We demonstrate, for the first time, that APAP acutely increases P-gp activity by a CAR-dependent mechanism. Furthermore, this increase in P-gp activity is associated with significantly reduced brain accumulation of morphine and reduced analgesic efficacy in animals administered morphine following APAP dosing. These are critical findings that point toward clinically significant drug-drug interactions.

Materials and Methods

PSC 833 (6-[(2*S*,4*R*,6*E*)-4-methyl-2-(methylamino)-3-oxo-6-octenoic acid]-7-L-valine-cyclosporin A; valspodar) was obtained from Tocris Bioscience (Minneapolis, MN). APAP, PB, dimethyl sulphoxide (DMSO), actinomycin D (Act D), CsA, okadaic acid (OA), the mouse monoclonal anti-actin antibodies, and the rabbit polyclonal anti–von Willebrand factor antibodies were purchased from Sigma-Aldrich (St. Louis, MO). BODIPY-verapamil hydrochloride was purchased from Life Technologies (Carlsbad, CA). The rabbit polyclonal anti-CAR antibody was purchased from Abcam (San Francisco, CA). The goat polyclonal anti–lamin B antibody (M-20) was obtained from Santa Cruz Biotechnology (Dallas, TX), and the mouse monoclonal anti–P-gp antibody (C219) was purchased from ID Laboratories (London, ON, Canada).

Animals and Treatments. All animal experiments were approved by the University of Arizona Institutional Animal Care and Use Committee and conformed to National Institutes of Health guidelines. Female Sprague-Dawley rats (200–250 g) were purchased from Harlan Sprague-Dawley (Indianapolis, IN), housed under standard 12-hour light/dark conditions, and provided with food and water ad libitum. Female rats were selected to maintain consistency with previous work (Seelbach et al., 2007; Ronaldson et al., 2011). Additionally, female rodents are preferable to males for transport studies since androgens have been shown to repress functional expression of ATP-binding cassette transporters (Cui et al., 2009). APAP (250 and 500 mg/kg) was prepared in 100% DMSO. PB (80 mg/kg) was prepared in a 50:50 ethanol:water solution. OA (0.1 ng/kg injected to obtain 2 nM plasma concentration) was prepared in 100% DMSO. Act D (79.5 mg/kg injected to obtain 1 μM plasma concentration) was prepared in 0.9% saline. All of these drug concentrations were based on the total blood volume of a 250-g rat. Total blood volume can be determined by the equation of Lee and Blaufox: [blood volume (ml) = 0.06 $\times$ body weight (g) + 0.77], which yields a blood volume of 15.77 ml (Ronaldson et al., 2009). APAP and PB were administered by i.p. injection to female Sprague-Dawley rats at selected time points (i.e., 1, 3, 6, or 24 hours) prior to microvessel isolation or in situ brain perfusion. OA and Act D were administered by i.p. injection 1 hour prior to APAP or PB treatment. Vehicle control animals were administered either 1 μl/g 100% DMSO or 0.9% saline by i.p. injection.

Microvessel Isolation. Brain microvessels were harvested as previously described by our laboratory (Seelbach et al., 2007; Campos et al., 2008; Ronaldson et al., 2009, 2011). Briefly, following anesthesia with sodium pentobarbital (64.8 mg/ml i.p.), rats were decapitated and brains removed. The meninges and choroid plexus were excised and the cerebral hemispheres were homogenized in 4 ml of microvessel isolation buffer (103 mM NaCl, 4.7 mM KCl, 2.5 mM $CaCl_2$, 1.2 mM KH_2PO_4, 1.2 mM $MgSO_4$, 15 mM HEPES, pH 7.4) containing protease inhibitor cocktail (Sigma-Aldrich). At this time, 8 ml of 26% dextran at 4°C was added to the homogenate and vortexed. Homogenates were then centrifuged (5600*g*; 4°C) for 10 minutes and the supernatant was aspirated. Pellets were resuspended in 10 ml of microvessel isolation buffer and passed through a 70-μm filter (Becton Dickinson, Franklin Lakes, NJ). Filtered homogenates were pelleted by centrifugation at 3000*g* for 10 minutes. At this time, the supernatant was aspirated and the pellet was collected for use in Western blot analyses or for preparation of cellular fractions. Cytoplasmic and nuclear fractions were isolated using the Qproteome Cell Compartment Kit (Qiagen, Germantown, MD) according to the manufacturer's instructions. Crude membrane preparations were obtained by resuspending the pellet in a modified radioimmunoprecipitation buffer consisting of 50 mM Tris HCl, pH 7.4, 150 mM NaCl, 1.0 mM EGTA, 1.0 mM sodium *o*-vanadate, 1% (v/v) Nonidet P-40, 0.25% (m/v) sodium deoxycholate, 0.1% (m/v) SDS, 200 μM phenylmethylsulfonyl fluoride, and 0.1% protease inhibitor cocktail (Sigma-Aldrich). The cells were gently rocked for 15 minutes at 4°C to allow lysis to occur. Lysates were then centrifuged (3000*g*; 4°C) for 10 minutes. Denucleated supernatants were centrifuged at 100,000*g* (4°C) for 60 minutes. Pellets (i.e., crude membranes) were resuspended in phosphate-buffered saline–containing protease inhibitor cocktail and frozen at −20°C until future use.

Western Blot Analysis. Protein isolated from rat brain microvessels was quantified using the bicinchoninic acid protein assay (Pierce Biotechnology, Rockford, IL) and analyzed for expression of CAR and P-gp. Microvessel protein samples (10 μg) were resolved on 10% SDS–polyacrylamide gels (Bis-Tris Criterion XT; Bio-Rad, Hercules, CA) and transferred to a polyvinylidene difluoride membrane. Protein transfer was verified by Ponceau S staining, and polyvinylidene difluoride membranes were incubated in Superblock

(Pierce Biotechnology) containing 0.05% (v/v) Tween-20 overnight at 4°C. Membranes were then incubated with primary antibody: rabbit polyclonal anti-CAR (1:750 dilution), mouse monoclonal anti–P-gp C219 (1:2000 dilution), goat polyclonal anti–lamin B M-20 (1:1000 dilution), or mouse monoclonal anti-actin AC40 (1:2000 dilution) overnight at 4°C. The membranes were then washed in Tris-buffered saline/Tween 20 (six times for 5 minutes each) and incubated with appropriate secondary antibodies for 1 hour at room temperature. Membranes were developed using enhanced chemiluminescence (ECL, Amersham, Piscataway, NJ). Membranes were stained for total protein with Ponceau S and the optical density of each band was normalized to total protein in each sample (i.e., loading control) according to a previously published method (Romero-Calvo et al., 2010). Ponceau S staining has long been applied for quality control of membrane transfer and is often used as an alternative to individual housekeeping/structural proteins (i.e., actin, glyceraldehyde-3-phosphate dehydrogenase) in assessment of equal loading in Western blots. Ponceau S is a fast and a fully reversible stain that, when applied and quantified prior to antibody staining, has been validated as an alternative means to immunoblotting of individual specific proteins for assessment of protein loading during Western blot analysis (Romero-Calvo et al., 2010). Since experimental manipulations (i.e., drug treatment) have been shown to alter expression of housekeeping proteins (i.e., actin, glyceraldehyde-3-phosphate dehydrogenase) (Aldridge et al., 2008) and homogenate concentrations that allow for detection of our low-abundance proteins of interest (i.e., P-gp and CAR) put high-abundance loading control proteins outside the linear range of detection (Dittmer and Dittmer, 2006), we chose to use total protein as our loading control. Bands were quantitated and corrected for background using ImageJ densitometric software (Wayne Rasband, Research Services Branch, National Institute of Mental Health, Bethesda, MD). All data were normalized to saline control values that were matched to treated animals from the same experimental day and reported as percent of control (%control).

Confocal Microscopy. Immunofluorescence of rat brain microvessels (isolated as described above) was performed as previously described (Lochhead et al., 2010). Briefly, brain microvessels were incubated on glass slides at room temperature for 15 minutes to enable vessel adherence. This was followed by fixation in 4% paraformaldehyde for 10 minutes. The slides were blocked in 2% goat serum and 1% bovine serum albumin before incubation in C219 antibody (1:100) and rabbit polyclonal antibody directed against von Willebrand factor (1:5000), an established brain microvessel marker. Slides were incubated in the presence of both primary antibodies for 90 minutes at room temperature. All slides were then incubated with appropriate Alexa Fluor-conjugated secondary antibodies (i.e., Alexa Fluor 488 goat anti-mouse IgG, Alexa Fluor 568 goat anti-rabbit IgG; Invitrogen, Carlsbad, CA) for 60 minutes at room temperature in the dark. All slides from control and treated rats were collected and processed in parallel. Primary antibody was omitted from slides in each treatment group as a negative control. All slides were imaged sequentially on a Leica SP5-II resonant scanner confocal microscope (Leica Microsystems, Buffalo Grove, IL) using a 40×/1.25 numerical aperture PL Apo oil-immersion objective lens. Filters were appropriately set to avoid bleed-through and to enhance the signal-to-noise ratio for each fluorophore. Images were obtained with a resolution of 2048 × 2048 and a pixel size of 0.11 μm. Semiquantitative analysis of the mean fluorescent intensity of P-gp was performed according to a previously published method (Hawkins et al., 2004). Microvessels were randomly chosen from rats in each treatment group, and the mean fluorescence intensity was analyzed from Leica Confocal Microscope image analysis software (Leica Microsystems) with the data presented as %control. Background correction settings were the same for all images acquired to ensure that data could be accurately compared between treatment groups.

Ex Vivo Fluorescent Transport Assay. Our ex vivo P-gp transport assay was performed as previously described (Bauer et al., 2004, 2006) with few modifications. Briefly, meninges, choroid plexus, and white matter of six brains (per treatment group) were excised and cerebral hemispheres were homogenized in 20 ml of capillary buffer (136.9 mM NaCl, 8.1 mM Na_2HPO_4, 2.7 mM KCl, 1.5 mM KH_2PO_4, 1 mM $CaCl_2$, 0.5 mM $MgCl_2$, 5 mM D-glucose, and 1 mM Na^+ pyruvate). Ficoll solution (30%) was then added to the homogenate at a volume of 40 ml, which was shaken and centrifuged (6000*g*; 4°C). Pellets were resuspended in 1 ml of 1% bovine serum albumin capillary buffer and loaded onto a glass bead column. Capillary buffer containing 1% bovine serum albumin was used as wash buffer, and elution was carried out by agitation of glass beads in capillary buffer. Glass beads were removed via filtration and the remaining buffer was then centrifuged (500*g*; 4°C). The resultant pellet was washed by resuspension in capillary buffer and centrifuged (6000*g*; 4°C). The pellet was then resuspended in 400 μl capillary buffer and plated onto chambered borosilicate cover glass. Adhered brain capillaries were then incubated for 30 minutes in the presence or absence of PSC 833 (5 μM) followed by incubation with the fluorescent P-gp substrate BODIPY-verapamil (1 μM) before visualization utilizing a Leica HCS A Inverted Confocal Microscope. In this assay, brain microvessels remained viable for at least 4 hours following removal from rat brain (Wang et al., 2010). Luminal fluorescent intensity was determined using ImageJ software (NIH, Bethesda, MD).

In Situ Brain Perfusion. In situ perfusion studies were carried out in female Sprague-Dawley rats (200–250 g) as previously described by our group (Seelbach et al., 2007; Ronaldson et al., 2009, 2011). Briefly, 3 hours post-APAP or PB treatment, animals were anesthetized with sodium pentobarbital (64.8 mg/ml i.p.) and heparinized (10,000 U/kg i.p.). Body temperature was maintained at 37°C using a heating pad. The common carotid arteries were cannulated with silicone tubing connected to a perfusion circuit. The perfusate was an erythrocyte-free modified mammalian Ringer's solution consisting of 117 mM NaCl, 4.7 mM KCl, 0.8 mM $MgSO_4$, 1.2 mM KH_2PO_4, 2.5 mM $CaCl_2$, 10 mM D-glucose, 3.9% (w/v) dextran (mol. wt. 60,000), and 1.0 g/l bovine serum albumin (type IV), pH 7.4, warmed to 37°C and oxygenated with 95% O_2/5% CO_2. Evan's blue dye (55 mg/l) was added to the perfusate to serve as a visual marker of BBB integrity. Perfusion pressure and flow rate were maintained at 95–105 mm Hg and 3.1 ml/min, respectively. Both jugular veins were severed to allow for drainage of the perfusate. Using a slow-drive syringe pump (0.5 ml/min per hemisphere; Harvard Apparatus, Holliston, MA), [^{3}H]morphine (0.5 μCi/ml) was added to the inflowing perfusate. Following perfusion, the rat was decapitated and the brain was removed. The meninges and choroid plexus were excised and cerebral hemispheres were sectioned and homogenized. TS2 tissue solubilizer (1 ml) was added to each tissue sample and the samples were allowed to solubilize for 2 days at room temperature. To eliminate chemiluminescence, 100 μl of 30% glacial acetic acid was added, along with 2 ml Optiphase SuperMix liquid scintillation cocktail (PerkinElmer, Boston, MA). Samples were measured for radioactivity on a model 1450 liquid scintillation counter (PerkinElmer). For inhibition studies, animals were perfused with erythrocyte-free modified mammalian Ringer's solution containing a P-gp inhibitor (i.e., 10 μM CsA, 5 μM PSC 833) for 10 minutes prior to perfusion with [^{3}H]morphine.

Results were reported as picomoles of radiolabeled morphine per gram of brain tissue (*C*; pmol/g tissue), which is equal to the total amount of radioisotope in the brain [C_{Brain}; dpm/g tissue] divided by the amount of radioisotope in the perfusate [$C_{Perfusate}$; dpm/pmol]: $C = C_{Brain}/C_{Perfusate}$. The brain vascular volume in rats has been previously shown to range between 6 and 9 μl/g brain tissue (Takasato et al., 1984). Since brain tissue was processed immediately after perfusion with a radiolabeled substrate, all uptake values required correction for brain vascular volume. This was accomplished by subtracting the average vascular volume [i.e., 8.0 μl/g brain tissue as calculated from data reported by Takasato and colleagues (1984)] from whole-brain uptake data obtained using [^{3}H]morphine. Multiple time uptake data were best-fit to a nonlinear least squares regression model, using the following equation: $C = (K_{in}/k_{out}) \times (1 - e^{-k(out)T})$, where *C* is the concentration of drug per gram of brain tissue, T is time

in minutes, K_{in} is the calculated uptake transfer constant, and k_{out} is the brain efflux rate coefficient estimated. The estimated brain volume of distribution (V_{Br}) was calculated using the following equation: $V_{Br} = K_{in}/k_{out}$. All kinetic parameters were calculated using SigmaPlot 11 graphical and statistical software (SPSS, Inc., Chicago, IL).

Antinociceptive Analysis. A warm-water (50°C) tail flick assay was used to measure the sensitivity of the tail to a noxious thermal stimulus. Specifically, this assay measured a spinally and supraspinally mediated antinociceptive response, which provided an index of BBB permeation for morphine, a peripherally administered opioid agonist (Vanderah et al., 2008). Animals were gently held around the trunk, and the distal 2/3 of the tail was immersed in a 50°C constant temperature, circulating warm-water bath. The latency to tail flick or withdrawal of the tail from the water was taken as the experimental end point with a cut-off of 10 seconds to avoid tissue damage. Baseline tail flick values were obtained prior to treatment (i.e., 2.84 ± 0.1 second). After baseline measurements were recorded, animals were administered (i.p.) one of the following: APAP (500 mg/kg) alone; morphine (10 mg/kg) alone; morphine (10 mg/kg) and APAP (500 mg/kg) concurrently; morphine (10 mg/kg) 3 hours post-APAP (500 mg/kg) treatment; or morphine (10 mg/kg) 6 hours post-APAP (500 mg/kg). Testing was performed 30, 45, 60, and 120 minutes postmorphine administration (or post-APAP administration in the APAP-alone group). Raw tail flick data were converted to area under the curve using the trapezoidal method to enable statistical comparisons between treatment groups.

Statistical Analysis. Western blot analysis data are reported as mean ± S.E.M. from at least three separate experiments where each treatment group consists of pooled microvessels from three animals. Confocal data are reported as mean ± S.E.M. from at least 50 brain capillaries per treatment group. Ex vivo transport assay data are reported as mean ± S.E.M. from three separate experiments where at least 50 brain capillaries were examined per treatment group. In situ brain perfusion data are reported as mean ± S.E.M. from six individual animals per treatment group. Antinociceptive analysis data are reported as mean ± S.E.M. from 10 individual animals per treatment group. To determine statistical significance between treatment groups in Western blot and confocal experiments, Student's t test was used for unpaired experimental data. To determine statistical significance between treatment groups in ex vivo transport experiments, Kruskal-Wallis one-way analysis of variance (ANOVA) on ranks and the post-hoc multiple-comparison Tukey's t test were used. To determine significance of brain [^{3}H]morphine accumulation, a repeated measures ANOVA and post-hoc multiple-comparison Bonferroni t test were used. To determine significance between treatment groups in tail flick experiments a two-way time versus treatment ANOVA and post-hoc multiple-comparison Holm-Sidak t test were used. A value of $P < 0.05$ was accepted as statistically significant.

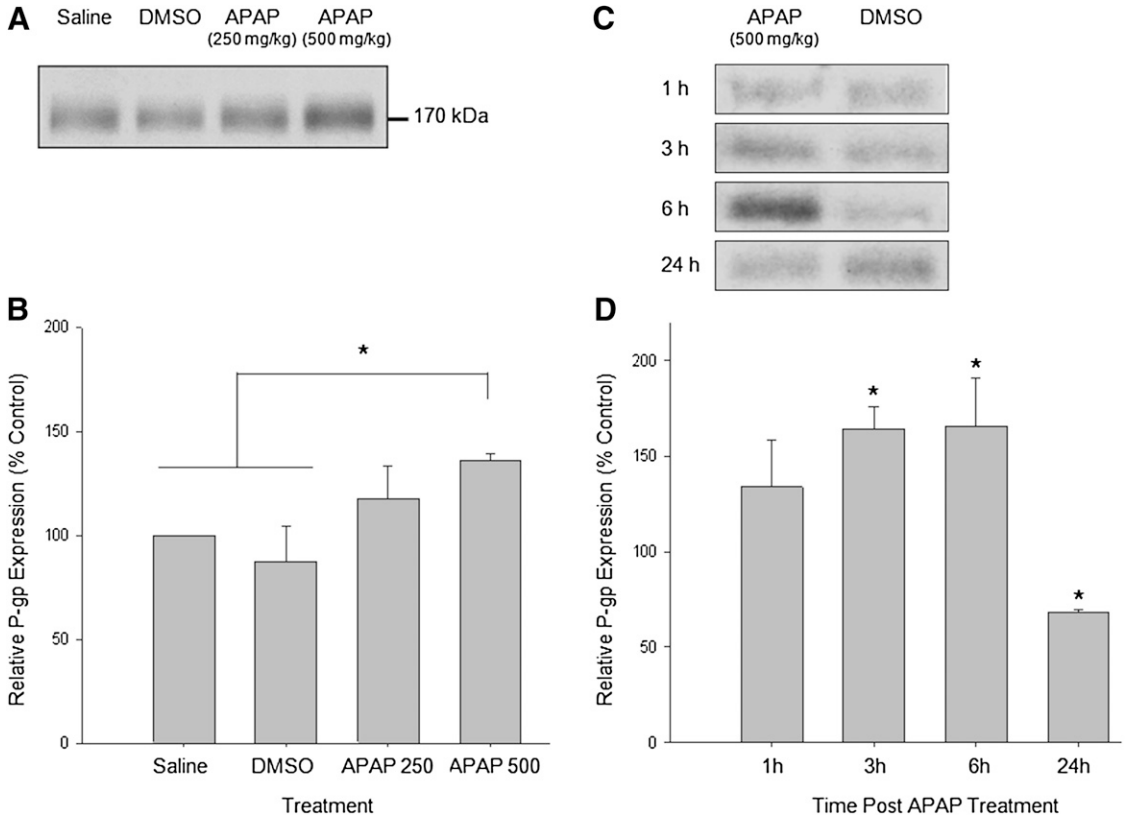

Fig. 1. APAP increases P-gp protein expression in a concentration-dependent manner. (A) Animals were administered (i.p.) a single injection of saline, DMSO (vehicle control), APAP 250 mg/kg, or APAP 500 mg/kg. After 3 hours, animals were sacrificed and brain microvessels were isolated and prepared for Western blot analysis. Whole microvessels (10 μg) were resolved on a 10% SDS-polyacrylamide gel and transferred to a polyvinylidene difluoride membrane. Samples were analyzed for expression of P-gp. (B) Relative levels of P-gp expression in samples from A were determined by densitometric analysis. Results are expressed as mean ± S.E.M. of three separate experiments (nine animals per group). Asterisks represent data points that are significantly different from control (*$P < 0.05$). (C) Animals were administered (i.p.) a single injection of DMSO or APAP 500 mg/kg. After 1, 3, 6, or 24 hours, animals were sacrificed and brain microvessels were isolated and prepared for Western blot analysis. Whole microvessels (10 μg) were resolved on a 10% SDS-polyacrylamide gel and transferred to a polyvinylidene difluoride membrane. Samples were analyzed for expression of P-gp. (D) Relative levels of P-gp expression in samples from C were determined by densitometric analysis. Results are expressed as mean ± S.E.M. of three separate experiments (nine animals per group). Asterisks represent data points that are significantly different from control (*$P < 0.05$).

Results

APAP Increases P-gp Protein Expression in Isolated Rat Brain Microvessels. To evaluate the effect of a single dose of APAP on P-gp protein expression, animals were administered APAP (i.p.) 3 hours prior to microvessel isolation. A 3-hour time point was selected based on the 2.6–3.6-hour in vivo half-life of APAP in the rat (Gonzalez-Martin et al., 1998). A known CAR-activating dose of APAP (500 mg/kg) and a suboptimal dose of APAP (250 mg/kg) were selected; 500 mg/kg, but not 250 mg/kg APAP has previously been shown to activate CAR in mice (Zhang et al., 2002). A single dose of APAP (500 mg/kg) significantly increased (1.4-fold) P-gp protein levels in whole microvessel homogenates as compared with homogenates from saline and DMSO vehicle control animals (Fig. 1, A and B). The 250 mg/kg APAP dose did not significantly increase P-gp expression. Additionally, P-gp expression in the DMSO vehicle control group did not significantly differ from that of the saline group. DMSO has previously been established as a vehicle control both in CAR induction studies (Burk et al., 2005) and in BBB transport studies in our own laboratory (Ronaldson et al., 2011). The 500 mg/kg APAP dose was used for all subsequent experiments because this dose generated a significant increase in P-gp expression. Furthermore, this dose of APAP is not associated with overt toxicity in Sprague-Dawley rats (Kim et al., 2007; McGill et al., 2012).

To investigate the time course of APAP's effect on P-gp expression, animals were administered APAP (500 mg/kg i.p.) or DMSO (i.p.) vehicle control 1, 3, 6, or 24 hours prior to microvessel isolation. In accordance with the dose-response data presented in Fig. 1, A and B, P-gp expression was found to be increased (1.6-fold) with APAP treatment at 3 hours, as compared with DMSO (Fig. 1, C and D). Additionally, P-gp expression was increased (1.6-fold) at 6 hours but was decreased at 24 hours (0.7-fold) following APAP treatment. All subsequent experiments were conducted at the 3-hour time point since this is where we detected the maximal increase in P-gp expression following a single APAP dose.

To further examine and visualize the effect of APAP on P-gp at the BBB, we examined P-gp expression using confocal microscopy. Our data show that P-gp staining along brain microvessels was enhanced 2-fold in APAP or PB-treated animals at 3 hours, as compared with microvessels from saline treated animals (Fig. 2). Taken together, these data suggest that APAP treatment modifies P-gp expression in rat brain microvessels.

APAP Increases P-gp–Mediated Transport in Ex Vivo P-gp Transport Assay. Since we observed an increase in P-gp expression following APAP treatment, we sought to determine if this corresponded to a change in P-gp transport activity. Therefore, activity of P-gp was assessed using an ex vivo P-gp transport assay. Animals were treated with 0.9% saline (1 ml/kg injection volume), APAP (500 mg/kg), or PB (80 mg/kg), a well-established CAR activator (Wang et al., 2010). Microvessels were isolated from animals and incubated with the fluorescent P-gp substrate BODIPY-verapamil in the presence or absence of the P-gp inhibitor PSC 833. Previous kinetic studies indicate that BODIPY-verapamil can be used as a probe substrate for P-gp (Lelong et al., 1991; Simmons et al., 1995). While BODIPY-verapamil is also a known substrate for multidrug resistance-associated protein 1 (Mrp1), recent studies suggest that Mrp1 is primarily localized to the abluminal (i.e., brain) aspect of the rodent BBB (Roberts et al., 2008). Therefore, Mrp1 is not expected to contribute to luminal BODIPY-verapamil accumulation. Microvessels from both PB- and APAP-treated animals showed significantly increased luminal fluorescence as compared with the microvessels isolated from saline-treated animals (Fig. 3). An increase in luminal fluorescence is representative of an increase in brain-to-blood (i.e., efflux) transport. In the presence of PSC 833, vessels

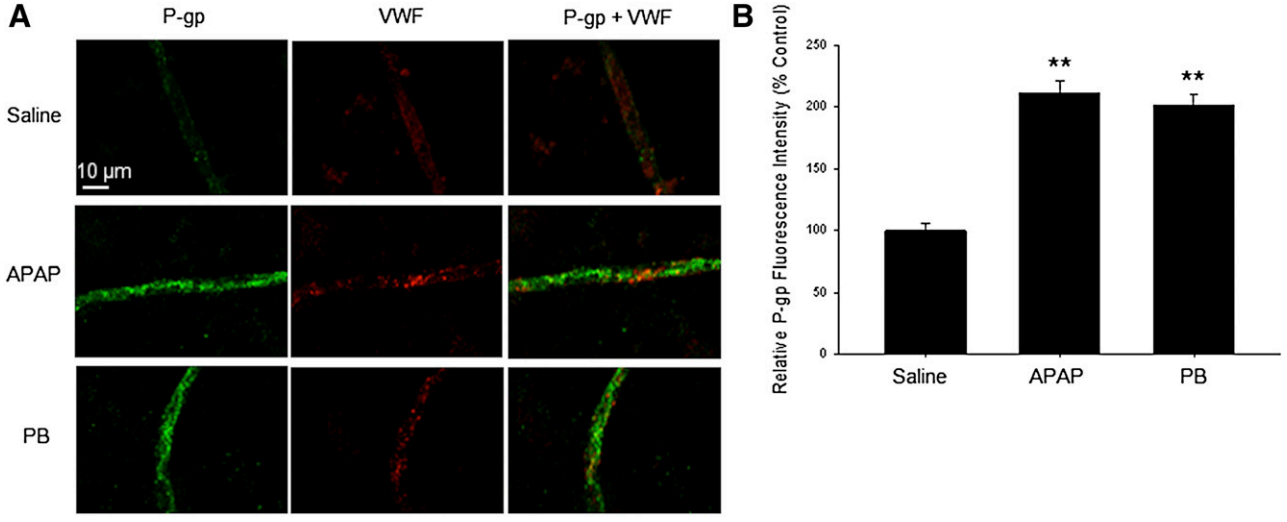

Fig. 2. APAP increases P-gp immunofluorescence. Animals were administered (i.p.) a single injection of saline, DMSO (vehicle control), or APAP 500 mg/kg. After 3 hours, animals were sacrificed and brain microvessels were isolated, plated on glass slides, fixed, and probed with mouse monoclonal anti–P-gp antibody and rabbit polyclonal antibody directed against von Willebrand factor (VWF). All slides were then incubated with appropriate Alexa Fluor–conjugated secondary antibodies. (A) Representative immunofluorescent images from animals treated with saline (top row), APAP (middle), or PB (bottom). Scale bar = 10 μm. (B) Semiquantitative analysis of the mean fluorescent intensity of P-gp. Microvessels isolated from treated and control animals were randomly selected for image analysis. Each bar represents the mean ± S.E.M. of 50 microvessels. Data are presented as percent of control. Asterisks represent data points that are significantly different from saline (**$P < 0.01$).

showed markedly reduced luminal fluorescence in each treatment group, suggesting involvement of P-gp in brain-to-blood transport of BODIPY-verapamil. Taken together, our data show that a single dose of APAP can modulate P-gp transport activity at the BBB.

Increased P-gp Expression/Transport Is CAR-Dependent. Since CAR has been shown to be a critical regulator of P-gp at the BBB (Wang et al., 2010; Chan et al., 2011), and APAP is a known CAR ligand (Zhang et al., 2002), we hypothesized that APAP may increase P-gp protein expression via activation of CAR. CAR is a nuclear receptor that is activated by ligand binding in the cytoplasm. Inactive CAR is sequestered within the cytoplasm by cytosolic binding proteins heat shock protein 90 and cytoplasmic CAR retention protein (Timsit and Negishi, 2007). Activating ligands recruit protein phosphatase 2A (PP2A) to the CAR–heat shock protein 90–cytoplasmic CAR retention protein complex, leading to dephosphorylation of threonine 38 in hCAR or threonine 48 in rodent CAR (Mutoh et al., 2009). Dephosphorylation leads to dissociation of cytosolic binding proteins and translocation of CAR to the nucleus. In the nucleus, CAR forms a heterodimer with retinoid X receptor, binds the phenobarbital-responsive enhancer module, and activates target gene transcription (Timsit and Negishi, 2007). Therefore, a change in the nuclear/cytoplasmic ratio for CAR is indicative of altered CAR-mediated signal transduction. One method of assessing activation of CAR is through comparison of CAR protein expression in the nucleus to that of CAR protein expression in the cytoplasm. To correlate expression levels of CAR with the potential for signal transduction, we calculated the nuclear/cytoplasmic ratio for CAR, as previously described (Ronaldson et al., 2009). For these experiments, microvessels from animals treated with APAP (500 mg/kg), PB (80 mg/kg), or saline were fractionated into cytoplasmic and nuclear compartments using the Qproteome cell fractionation kit (Qiagen). Western blotting and subsequent densitometric analysis were used to determine the level of CAR protein expression in the nucleus as compared with that in the cytoplasm. APAP and PB both significantly increased the nuclear to cytoplasmic ratio of CAR as compared with control (Fig. 4), suggesting activation of CAR.

The role of CAR signaling in the APAP-induced increase in P-gp transport was evaluated using two CAR pathway inhibitors: OA, a PP2A inhibitor, and Act D, a transcriptional inhibitor. OA blocks activation of CAR by inhibiting its dephosphorylation via PP2A (Pei et al., 2003). Act D blocks transcription by intercalating into DNA and preventing progression of RNA polymerases (Koba and Konopa, 2005). Animals were dosed with OA (0.1 ng/kg, to obtain 2 nM plasma concentration) or Act D (79.5 mg/kg, to obtain 1 μM plasma concentration) 1 hour prior to treatment with APAP (500 mg/kg), saline, or PB (80 mg/kg). These doses of inhibitors were selected based on previous studies that showed them to be

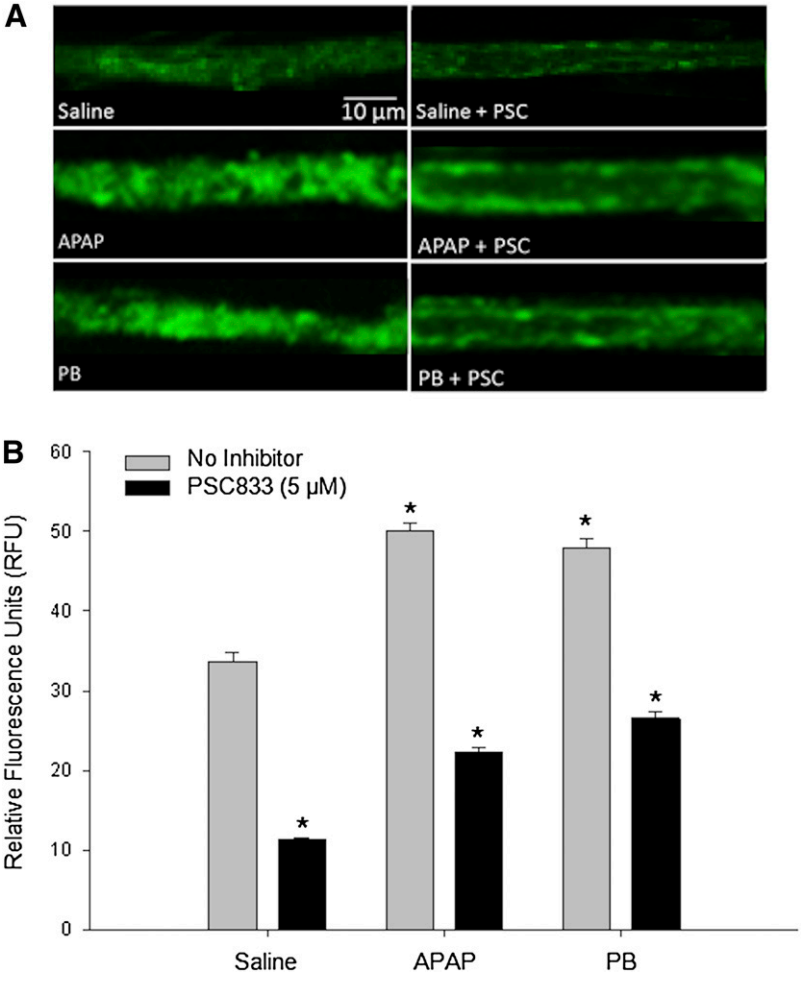

Fig. 3. Increased P-gp transport activity following treatment with APAP or PB. (A) Representative images show increased luminal accumulation of BODIPY-verapamil, an established P-gp substrate, following treatment with known CAR activators APAP and PB. Luminal fluorescence was significantly reduced in the presence of PSC 833 (PSC), an established P-gp inhibitor. Scale bar = 10 μm. (B) Quantification of luminal fluorescence shows that APAP- and PB-induced increases in P-gp transport activity are attenuated by the P-gp inhibitor PSC 833. Results are expressed as mean ± S.E.M. of at least 50 individual capillaries per group from two separate experiments. Asterisks represent data points that are significantly different from saline, unless otherwise indicated (*$P < 0.05$).

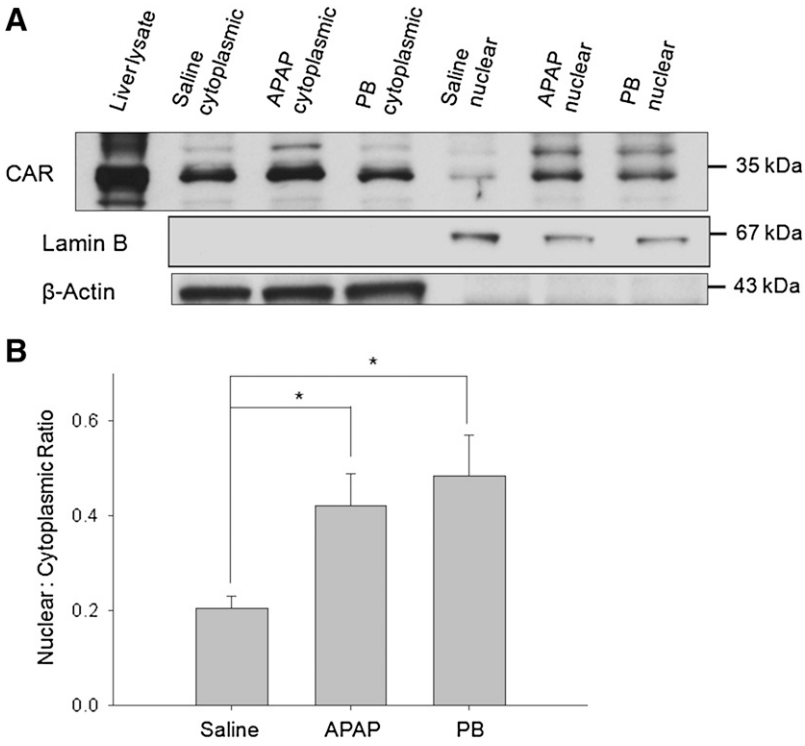

Fig. 4. Expression of CAR in brain microvessels following treatment with APAP or PB. (A) Western blot analysis of microvessels isolated from rats treated with 500 mg/kg APAP or 80 mg/kg PB for 3 hours. Cytoplasmic and nuclear extracts from rat brain microvessels (10 μg) were resolved on a 10% SDS-polyacrylamide gel and transferred to a polyvinylidene difluoride membrane. Samples were analyzed for expression of CAR. (B) Relative levels of CAR determined by densitometric analysis and the nucleus-to-cytoplasm ratio were calculated. Results are expressed as mean ± S.E.M. of three separate experiments. Asterisks represent data points that are significantly different from saline ($^*P < 0.05$).

effective in inhibiting CAR activation and CAR-induced transcription, respectively (Wang et al., 2010). OA and Act D treatment blocked the APAP- and PB-induced increases in P-gp expression in crude membrane preparations (Fig. 5), suggesting a dependence on dephosphorylation and transcription, respectively. In accordance with expression data, OA and Act D treatment significantly attenuated the increase in luminal BODIPY-verapamil fluorescence observed in vessels isolated from animals administered APAP or PB alone (Fig. 6). Consistent with previous work (Wang et al., 2010), OA did not affect

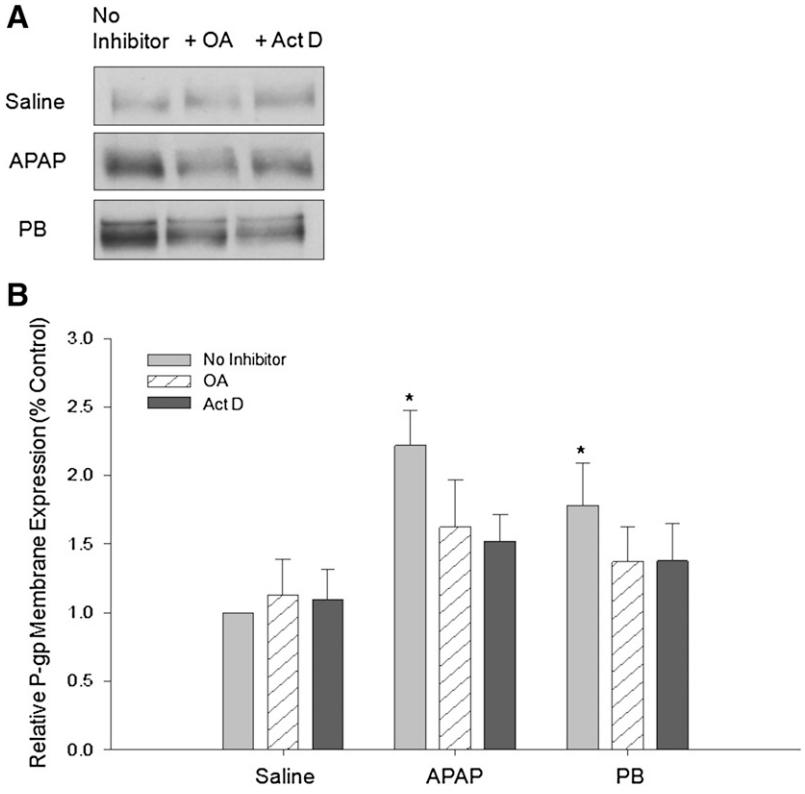

Fig. 5. APAP-induced increase in P-gp expression attenuated by protein phosphatase 2A/CAR pathway inhibitor OA and transcriptional inhibitor/CAR pathway inhibitor Act D. Animals were administered (i.p.) a single injection of OA or Act D 1 hour prior to administration of saline, APAP (500 mg/kg), or PB (80 mg/kg). After 3 hours, animals were sacrificed and brain microvessels were isolated. Crude membrane fractions were isolated and prepared for Western blot analysis. (A) Crude membrane fractions (10 μg) were resolved on a 10% SDS-polyacrylamide gel and transferred to a polyvinylidene difluoride membrane. Samples were analyzed for expression of P-glycoprotein. (B) Relative levels of P-gp expression in samples from control, OA-, or Act D–treated animals were determined by densitometric analysis. Results are expressed as mean ± S.E.M. of three separate experiments (nine animals per group). Asterisks represent data points that are significantly different from control ($^*P < 0.05$).

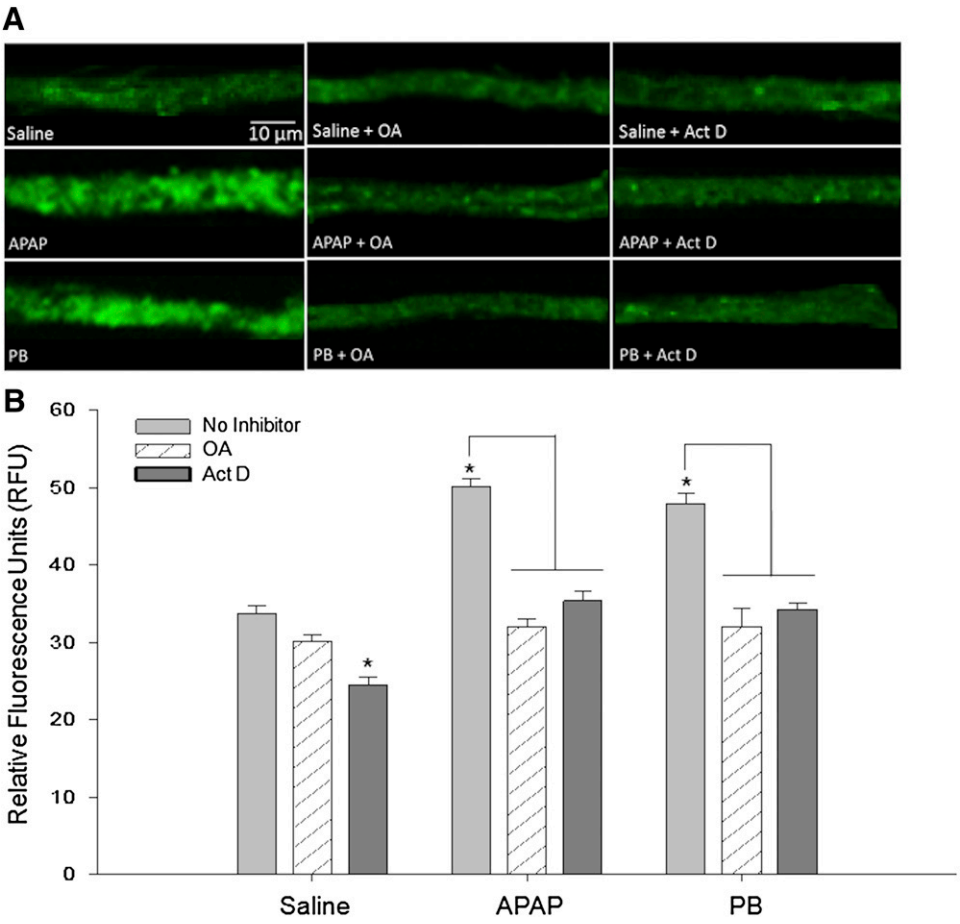

Fig. 6. APAP-induced increase in P-gp transport attenuated by protein phosphatase 2A/CAR pathway inhibitor OA and transcriptional inhibitor/CAR pathway inhibitor Act D. Animals were administered (i.p.) a single injection of OA or Act D 1 hour prior to administration of saline, APAP (500 mg/kg), or PB (80 mg/kg). After 3 hours, animals were sacrificed and brain microvessels were isolated and prepared for ex vivo transport assay. Scale bar = 10 μm. (A) Representative confocal images show decreased luminal accumulation of BODIPY-verapamil, an established P-gp substrate, following treatment with PP2A inhibitor OA or transcriptional inhibitor Act D. (B) Quantification of luminal fluorescence shows that APAP- and PB-induced increases in P-gp transport activity are attenuated by OA and Act D pretreatment. Results are expressed as mean ± S.E.M. of at least 50 individual capillaries per group from two separate experiments. Asterisks represent data points that are significantly different from saline, unless otherwise indicated (*$P < 0.05$).

BODIPY-verapamil transport while Act D treatment decreased P-gp activity in control vessels. Taken together, these data suggest a role for CAR in the regulation of P-gp transport activity at the BBB following exposure to APAP or PB.

BBB Permeability to Morphine Decreased Following APAP Treatment. To examine the functional relevance of APAP-induced P-gp upregulation, we investigated whether APAP pretreatment altered brain permeation of the established P-gp substrate morphine. In situ brain perfusion was used to determine whether APAP treatment altered blood-to-brain transport activity of the opioid. Brain [^{3}H]morphine uptake in saline-treated and APAP-treated animals showed increasing accumulation over the entire duration of the experiment (Fig. 7A). In APAP-treated animals, a significant decrease (2-fold) in [^{3}H]morphine uptake was observed compared with the uptake time course in saline controls. Multiple-time uptake data were fit using a nonlinear least squares regression equation: $C = (K_{in}/k_{out}) \times (1 - e^{-k(out)T})$, which provided R^2 values of 0.99 (saline) and 0.99 (APAP). Kinetic analysis of multiple-time uptake data revealed a significant increase ($P < 0.05$) in k_{out} and decrease in K_{in} ($P < 0.05$) in APAP-treated animals as compared with saline controls (Table 1), suggesting activation of an efflux process for morphine at the BBB. Of particular significance, the estimated brain volume of distribution at steady-state (V_{Br}) was reduced (1.6-fold) in APAP-treated animals as compared with saline controls, indicating reduced ability of morphine to permeate brain parenchyma.

To verify that observed changes in morphine-brain permeation were attributable to changes in P-gp transport, animals treated with APAP (500 mg/kg) or PB (80 mg/kg) were perfused at 3 hours in the presence or absence of P-gp inhibitors (i.e., 10 uM CsA, 5 uM PSC 833) for 10 minutes prior to perfusion with [^{3}H]morphine. P-gp inhibitors significantly increased [^{3}H]morphine accumulation in all groups (Fig. 7B). As with the APAP-treated animals, significantly less [^{3}H]morphine accumulated in the brains of PB-treated animals in the absence of a P-gp inhibitor. This effect was blocked by P-gp inhibitors CsA and PSC 833, further confirming P-gp involvement in decreased brain permeation of morphine following APAP treatment.

APAP Pretreatment Alters Morphine Antinociception. As there exists an inverse relationship between morphine analgesia and P-gp expression levels (Hamabe et al., 2007), we speculated that altered morphine brain permeation following APAP treatment could result in changes in morphine analgesia efficacy. A standard warm-water (50°C) tail flick assay was used to assess morphine analgesia following APAP treatment. In this established assay for opioid-induced analgesia, an increase in tail flick latency is indicative of an increased level of analgesia. Animals were administered (i.p.) either APAP (500 mg/kg) alone, morphine (10 mg/kg) alone, morphine and APAP concurrently, morphine 3 hours post-APAP treatment, or morphine 6 hours post-APAP treatment. The 3- and 6-hour time points were selected on the basis of Western blot data illustrating increased P-gp expression at

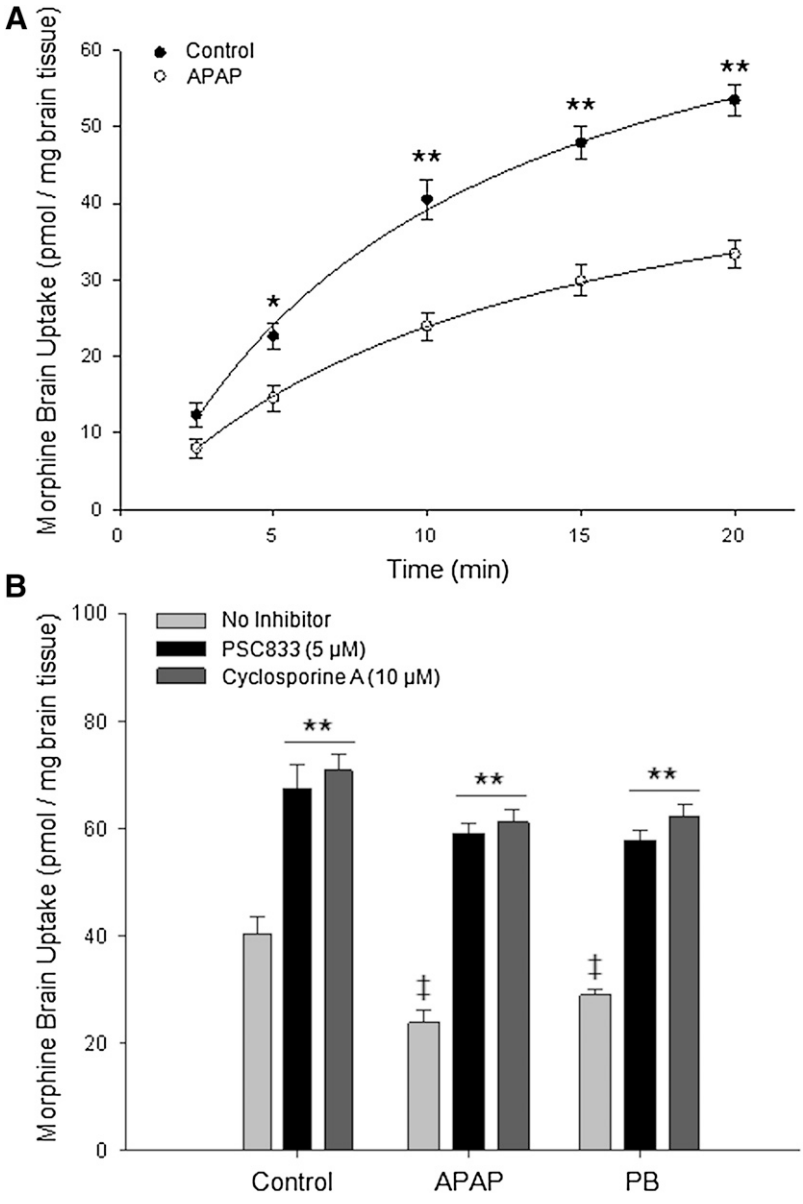

Fig. 7. Accumulation of [^{3}H]morphine into rat brain following APAP treatment. (A) Effect of APAP administration (3 hours) on the brain uptake of [^{3}H]morphine as determined by in situ brain perfusion. Animals were perfused with [^{3}H]morphine (0.5 mCi/ml) for 2.5, 5, 10, 15, and 20 minutes. Results are expressed as mean ± S.E.M. of six animals per time point. Multiple time data were best fit ($r^2 > 0.99$ for both treatment groups) using a nonlinear, least-squares regression model. Asterisks represent data points that were significantly different from control (saline-treated) animals (*$P < 0.05$; **$P < 0.01$). (B) Effect of P-gp inhibitors on the brain uptake of morphine during inflammatory pain. Animals were perfused with P-gp inhibitors (i.e., 10 μM CsA, 5 μM PSC 833) for 10 minutes prior to perfusion with [^{3}H]morphine. Animals were then perfused with [^{3}H]morphine (1.0 mCi/ml, 10 mM total concentration) for 10 minutes in the presence of the respective inhibitor. Results are expressed as mean ± S.E.M. of six individual animals per time point. Asterisks represent data points that were significantly different (**$P < 0.01$ from Control/No Inhibitor condition; $^‡P < 0.01$ from respective No Inhibitor condition).

these time points (see Fig. 1, C and D). APAP alone had no effect on tail flick latencies (no significant difference from baseline latencies) during the 30–120-minute time course or at 3 hours or 6 hours (data not shown). Morphine alone (30–120 minutes) exhibited increases in tail flick latencies that were directly comparable to previously published work (data not shown; Shen and Crain, 1997; Morgan et al., 2006). In accordance with previous findings for morphine (Shen and Crain, 1997), analgesia in all animals treated with morphine or morphine with APAP peaked 60 minutes postmorphine treatment (Fig. 8A). Two-way ANOVA showed a significant main effect for time ($F[3, 27] = 7.78$, $P < 0.001$); a significant main effect for treatment ($F[2, 27] = 3.86$, $P < 0.05$); and no time-treatment interaction ($F[1,27] = 0.26$, $P > 0.05$). Post-hoc comparisons using Holm-Sidak t tests revealed differences between animals treated with morphine and APAP concurrently and those treated with morphine 3 or 6 hours post-APAP administration. Area under the curve, a measure of total antinociception, was decreased in the 3-hour post-APAP group as compared with the concurrent administration group (Fig. 8B). While not statistically significant, a similar trend was evident between the concurrent administration group and the 6-hour post-APAP group. Taken together, these results suggest that animals administered morphine at 3 or 6 hours after APAP treatment, when P-gp levels are known to be elevated, experienced less analgesia than animals treated with the two drugs concurrently.

TABLE 1
Kinetic analysis of brain morphine uptake following APAP treatment
Results are expressed as mean ± S.D.

	Control	APAP
V_{Br}	63.83 ± 3.42 pmol/g	39.78 ± 0.36 pmol/g**
K_{in}	5.74 ± 0.46 pmol/g·min	4.77 ± 0.51 pmol/g·min*
k_{out}	0.09 ± 0.01/min	0.12 ± 0.01/min*

**$P < 0.01$; *$P < 0.05$.

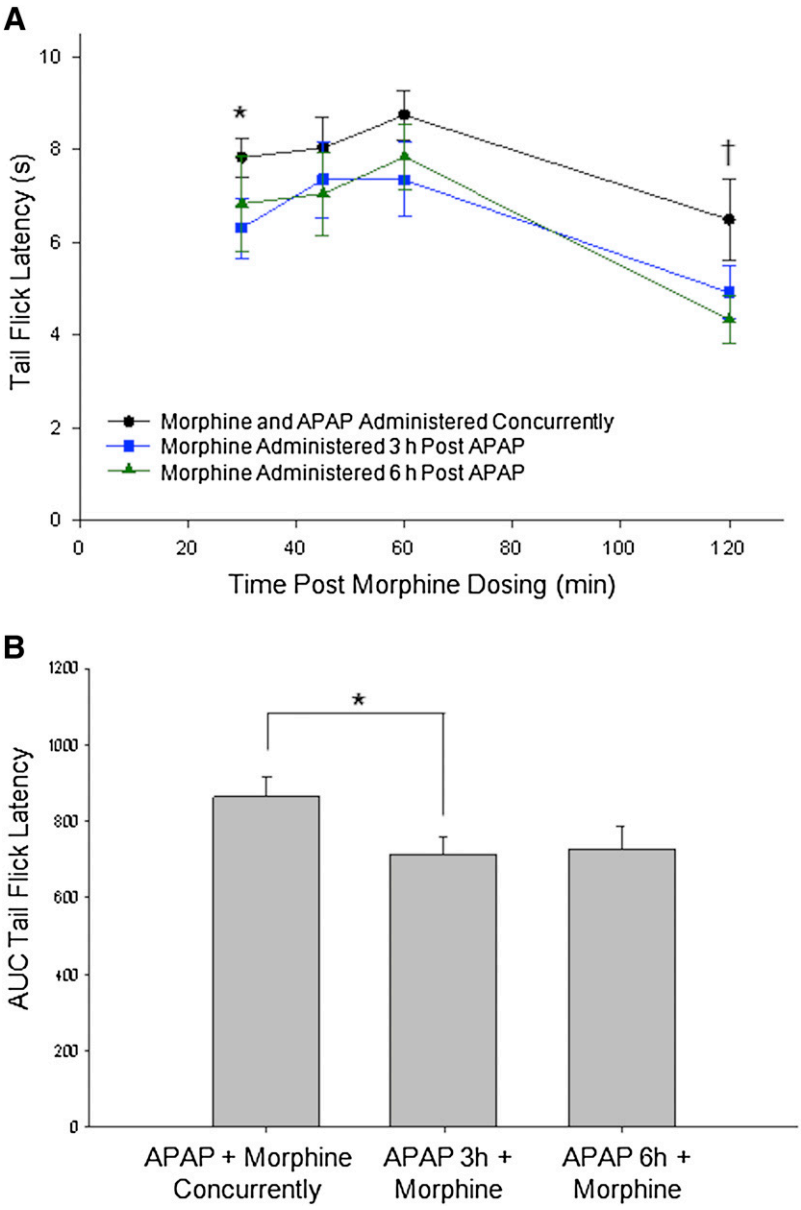

Fig. 8. APAP pretreatment alters morphine antinociception in warm-water (50°C) tail flick assay. Effect of APAP (500 mg/kg) administration on morphine (10 mg/kg) antinociception was assessed by hot-water tail flick. (A) Time-effect curves showing an increase in tail flick latency that peaks 60 minutes postmorphine dosing and is declining by 120 minutes. Two-way ANOVA indicates a decrease in morphine-induced analgesia in animals that received morphine 3 or 6 hours post-APAP treatment, as compared with animals that received both morphine and APAP concurrently. Results are expressed as mean ± S.E.M. of 10 animals per treatment group. $^{*}P < 0.05$ concurrent group versus 3-hour group; $^{\dagger}P < 0.05$ concurrent group versus 6-hour group. (B) Histogram bars represent areas under the time-effect curves illustrated in A. Asterisks represent data points that are significantly different ($^{*}P < 0.05$).

Discussion

At the BBB, P-gp restricts entry of endogenous substrates (i.e., steroids, cytokines, bilirubin) into brain parenchyma in an effort to precisely control their CNS concentrations (Demeule et al., 2002). P-gp also limits CNS xenobiotic permeation and is a constraining factor for effective drug delivery and/or treatment of neurologic diseases, including pain. It is well established that P-gp can modulate the disposition of opioids into the CNS (Hassan et al., 2009). For example, pharmacologic inhibition studies in P-gp–competent rodents and experimentation in P-gp–deficient [*mdr1a*(−/−)] mice have shown that P-gp can restrict CNS permeation and modulate antinociceptive activities of several opioid analgesic drugs, including morphine, oxycodone, methadone, fentanyl, loperamide, and [D-penicillamine2, 5]enkephalin (Chen and Pollack, 1999; Letrent et al., 1999; Dagenais et al., 2004; Hassan et al., 2007; Seelbach et al., 2007).

P-gp expression/activity at the BBB can be directly regulated by pharmacologic agents. Many previous in vitro and in vivo studies have shown that drugs can either modulate their own transport by P-gp (Zastre et al., 2009; Yousif et al., 2012) or the transport of other P-gp substrates (Bauer et al., 2004, 2006; Wang et al., 2010; Chan et al., 2011). This consideration is critical in pharmacotherapy of pain where ancillary medications such as APAP are often combined with opioids as part of a therapeutic regimen. In the current study, we demonstrated, for the first time, that a single dose of APAP increases P-gp expression in isolated rat brain capillaries after only a single half-life (i.e., 3 hours). This elevation in P-gp expression is maintained for at least 6 hours following APAP administration and is absent 24 hours post-APAP administration. Additionally, we showed that this increase in P-gp expression at 3 hours corresponded to enhanced P-gp–mediated transport activity at the BBB. Evidence for increased P-gp–mediated transport included: 1) increased luminal fluorescence of BODIPY-verapamil in rat brain capillaries isolated from APAP-treated animals that could be

attenuated by PSC 833; 2) reduced brain uptake of morphine, an established P-gp substrate, in APAP-treated animals during in situ perfusion that could be prevented by P-gp inhibitors CsA and PSC 833; and 3) a decrease in V_{Br} and K_{in} as well as an increase in k_{out} for morphine following APAP treatment, reflecting enhanced brain-to-blood morphine transport. Taken together, these data indicate, for the first time, that a single APAP dose can enhance P-gp–mediated transport processes at the BBB even at 3 and 6 hours after APAP treatment.

To fully understand the implications of APAP-mediated induction of P-gp activity, it is necessary to identify and characterize biologic mechanisms that enable drugs to modify endogenous BBB transport processes. APAP has been shown to be an activator of CAR (Zhang et al., 2002), a nuclear receptor involved in regulation of xenobiotic metabolism and elimination. CAR activation leads to transcription of genes that encode drug metabolizing enzymes and drug transporters (i.e., P-gp, MRP2, BCRP) (Burk et al., 2005; Kodama and Negishi, 2006; Wang et al., 2010; Chan et al., 2011). Of particular importance to this study, CAR activation has been shown to increase MDR1 expression in human colon adenocarcinoma cells (Burk et al., 2005) and P-gp expression and activity at the rodent BBB (Wang et al., 2010). While responses of nuclear receptors are characterized by marked interspecies differences, it is critical to emphasize that APAP activates both rodent CAR and hCAR (Zhang et al., 2002). This observation is particularly important because it points toward a mechanism that can be effectively studied in an in vivo rodent model system. Furthermore, this mechanism can be used to evaluate potential drug-drug interactions between APAP and P-gp substrate drugs (e.g., opioid analgesics) that may have profound clinical implications.

As CAR translocates to the nucleus upon activation, a change in the nuclear/cytoplasmic ratio for CAR is indicative of altered CAR-mediated signal transduction. In the present study, we observed increased nuclear/cytoplasmic ratio of CAR expression in both APAP- and PB-treated animals, suggesting activation of CAR-mediated signaling by these two ligands. We further evaluated the role of CAR in regulation of P-gp at the BBB using two CAR pathway inhibitors (i.e., OA and Act D). We observed that OA treatment prior to APAP administration attenuated the increase in luminal BODIPY-verapamil fluorescence observed in animals treated with APAP or PB. Furthermore, pretreatment with Act D before administration of APAP or PB also prevented changes in luminal BODIPY-verapamil fluorescence. Taken together, these data provide evidence for involvement of a CAR-dependent mechanism in the in vivo upregulation of P-gp expression and activity triggered by APAP.

Given that APAP increases P-gp at the BBB and the inverse relationship between morphine analgesia and P-gp expression levels (Hamabe et al., 2007), we assessed whether attenuated morphine brain permeation following APAP treatment resulted in modified morphine analgesic efficacy in a standard warm-water (50°C) tail flick assay. We measured differences in morphine analgesia in three experimental groups: 1) animals administered morphine and APAP concurrently, 2) animals administered morphine 3 hours post-APAP treatment, and 3) animals administered morphine 6 hours post-APAP treatment. Our data indicate that an increase in P-gp functional expression occurs 3 hours and 6 hours following a single APAP dose. Indeed, tail flick latency scores (in seconds) reveal a significant decrease in morphine-induced analgesia in animals that received morphine 3 or 6 hours after APAP treatment, as compared with those that received the two drugs concurrently. This finding has important clinical implications for the use of APAP and morphine together in pain management, as APAP is often given hours prior to morphine or coadministered (Remy et al., 2005). As described below, this observation is also in accordance with clinical evidence that suggests that APAP may modify morphine brain delivery.

The rodent APAP dose of 500 mg/kg used in this study corresponds to a Human Equivalent Dose of 5.67 g/d (U.S. Department of Health and Human Services, 2005; http://www.fda.gov/downloads/Drugs/Guidances/UCM078932.pdf). This is equal to a high therapeutic dose for humans (>4–6 g/d) (Albertson et al., 2010) and, thus, is often administered to patients receiving APAP for pain management. Such an APAP dose has the potential to activate CAR and increase P-gp functional expression at the BBB, an effect that may lead to significant drug-drug interactions. In fact, APAP and morphine are commonly used concurrently for management of postsurgical pain (Remy et al., 2005). Since our data imply that less morphine enters the brain in the presence of APAP, coadministration of morphine and APAP may require changes in morphine dose levels to achieve an analgesic effect that is similar to that achieved with morphine alone (i.e., contribute to morphine tolerance). Studies here did not attempt to examine a model of inflammation due to the fact that our previous studies (Seelbach et al., 2007; McCaffrey et al., 2008) demonstrated inflammation-induced BBB changes, including those that may increase BBB paracellular permeability and compromise BBB integrity (McCaffrey et al., 2008). As such, the combination of morphine and APAP during times of injury may initially be offset by inflammation-induced opening of the BBB. Long-term/chronic effects of sustained APAP use on opioid BBB penetration should be examined. Additionally, modified morphine brain permeation may result in altered incidence of adverse effects (e.g., addiction, nausea, respiratory depression). Indeed, a randomized, double-blind clinical study of patients undergoing dental surgery found that, acutely, APAP reduced the incidence of morphine-related adverse events (Van Aken et al., 2004). The data of Van Aken and colleagues may be the result of altered CNS morphine delivery induced by APAP. However, a recent mixed treatment comparison analysis of 60 relevant clinical studies reported that APAP reduced the amount of morphine required by patients to manage pain in the first 24 hours following major surgery (Maund et al., 2011). This morphine-sparing effect was only studied acutely and is not found in all patient populations (i.e., young infants) or following all procedures (i.e., lumbar laminectomy and discectomy, cesarean delivery) (Siddik et al., 2001; van der Marel et al., 2007; Cakan et al., 2008). Taken together, the results of these studies may reflect, in part, altered CNS delivery of morphine as a result of prior or concurrent APAP exposure over time. Repeated dosing often leads to analgesic tolerance that may be explained, in part, by changes in P-gp at the BBB, as noted here. The present study and clinical observations highlight the complexity of pain polypharmacy and emphasize the need for novel, translational studies assessing the effect of APAP and morphine coadministration. Studies evaluating effects of chronic APAP exposure on acute morphine brain permeation

and long-term morphine requirement for pain management are needed.

In summary, we describe, for the first time, increased functional expression of P-gp at the BBB after a single dose of APAP. We also demonstrate that activation of CAR directly modulates P-gp activity at the BBB, which alters morphine brain permeation and efficacy. Overall, these data demonstrate that CAR activation is a factor that contributes to drug-drug interactions involving APAP and opioids, an observation critical to the future of efficacious pain pharmacotherapy.

Authorship Contributions

Participated in research design: Slosky, Thompson, Sanchez-Covarrubias, Vanderah, Ronaldson, Davis.

Conducted experiments: Slosky, Thompson, Sanchez-Covarrubias, Zhang, Laracuente, Vanderah, Ronaldson.

Performed data analysis: Slosky, Thompson, Vanderah, Ronaldson, Davis.

Wrote or contributed to the writing of the manuscript: Slosky, Thompson, Vanderah, Ronaldson, Davis.

References

Albertson TE, Walker VM, Jr, Stebbins MR, Ashton EW, Owen KP, and Sutter ME (2010) A population study of the frequency of high-dose acetaminophen prescribing and dispensing. *Ann Pharmacother* **44**:1191–1195.

Aldridge GM, Podrebarac DM, Greenough WT, and Weiler IJ (2008) The use of total protein stains as loading controls: an alternative to high-abundance single-protein controls in semi-quantitative immunoblotting. *J Neurosci Methods* **172**:250–254.

Bauer B, Hartz AMS, Fricker G, and Miller DS (2004) Pregnane X receptor up-regulation of P-glycoprotein expression and transport function at the blood-brain barrier. *Mol Pharmacol* **66**:413–419.

Bauer B, Yang X, Hartz AM, Olson ER, Zhao R, Kalvass JC, Pollack GM, and Miller DS (2006) In vivo activation of human pregnane X receptor tightens the blood-brain barrier to methadone through P-glycoprotein up-regulation. *Mol Pharmacol* **70**: 1212–1219.

Burk O, Arnold KA, Geick A, Tegude H, and Eichelbaum M (2005) A role for constitutive androstane receptor in the regulation of human intestinal MDR1 expression. *Biol Chem* **386**:503–513.

Butt AM, Jones HC, and Abbott NJ (1990) Electrical resistance across the blood-brain barrier in anaesthetized rats: a developmental study. *J Physiol* **429**:47–62.

Cakan T, Inan N, Culhaoglu S, Bakkal K, and Başar H (2008) Intravenous paracetamol improves the quality of postoperative analgesia but does not decrease narcotic requirements. *J Neurosurg Anesthesiol* **20**:169–173.

Campos CR, Ocheltree SM, Hom S, Egleton RD, and Davis TP (2008) Nociceptive inhibition prevents inflammatory pain induced changes in the blood-brain barrier. *Brain Res* **1221**:6–13.

Chan GNY, Hoque MT, Cummins CL, and Bendayan R (2011) Regulation of P-glycoprotein by orphan nuclear receptors in human brain microvessel endothelial cells. *J Neurochem* **118**:163–175.

Chen C and Pollack GM (1999) Enhanced antinociception of the model opioid peptide [D-penicillamine] enkephalin by P-glycoprotein modulation. *Pharm Res* **16**: 296–301.

Chen CJ, Chin JE, Ueda K, Clark DP, Pastan I, Gottesman MM, and Roninson IB (1986) Internal duplication and homology with bacterial transport proteins in the mdr1 (P-glycoprotein) gene from multidrug-resistant human cells. *Cell* **47**:381–389.

Cui YJ, Cheng X, Weaver YM, and Klaassen CD (2009) Tissue distribution, gender-divergent expression, ontogeny, and chemical induction of multidrug resistance transporter genes (Mdr1a, Mdr1b, Mdr2) in mice. *Drug Metab Dispos* **37**:203–210.

Dagenais C, Ducharme J, and Pollack GM (2001) Uptake and efflux of the peptidic delta-opioid receptor agonist. *Neurosci Lett* **301**:155–158.

Dagenais C, Graff CL, and Pollack GM (2004) Variable modulation of opioid brain uptake by P-glycoprotein in mice. *Biochem Pharmacol* **67**:269–276.

Dauchy S, Dutheil F, Weaver RJ, Chassoux F, Daumas-Duport C, Couraud PO, Scherrmann JM, De Waziers I, and Declèves X (2008) ABC transporters, cytochromes P450 and their main transcription factors: expression at the human blood-brain barrier. *J Neurochem* **107**:1518–1528.

Demeule M, Régina A, Jodoin J, Laplante A, Dagenais C, Berthelet F, Moghrabi A, and Béliveau R (2002) Drug transport to the brain: key roles for the efflux pump P-glycoprotein in the blood-brain barrier. *Vascul Pharmacol* **38**:339–348.

Dittmer A and Dittmer J (2006) Beta-actin is not a reliable loading control in Western blot analysis. *Electrophoresis* **27**:2844–2845.

González-Martin G, Lyndon C, and Sunkel C (1998) Hepatic kinetics of SCP-1 (N-[alpha-(1,2-benzisothiazol-3(2H)-ona-1, 1-dioxide-2-yl)-acetyl]-p-aminophenol) compared with acetaminophen in isolated rat liver. *Eur J Pharm Biopharm* **46**: 293–297.

Gottesman MM, Hrycyna CA, Schoenlein PV, Germann UA, and Pastan I (1995) Genetic analysis of the multidrug transporter. *Annu Rev Genet* **29**:607–649.

Hamabe W, Maeda T, Kiguchi N, Yamamoto C, Tokuyama S, and Kishioka S (2007) Negative relationship between morphine analgesia and P-glycoprotein expression levels in the brain. *J Pharmacol Sci* **105**:353–360.

Hassan HE, Mercer SL, Cunningham CW, Coop A, and Eddington ND (2009) Evaluation of the P-glycoprotein (Abcb1) affinity status of a series of morphine analogs: comparative study with meperidine analogs to identify opioids with minimal P-glycoprotein interactions. *Int J Pharm* **375**:48–54.

Hassan HE, Myers AL, Lee IJ, Coop A, and Eddington ND (2007) Oxycodone induces overexpression of P-glycoprotein (ABCB1) and affects paclitaxel's tissue distribution in Sprague Dawley rats. *J Pharm Sci* **96**:2494–2506.

Hawkins BT, Abbruscato TJ, Egleton RD, Brown RC, Huber JD, Campos CR, and Davis TP (2004) Nicotine increases in vivo blood-brain barrier permeability and alters cerebral microvascular tight junction protein distribution. *Brain Res* **1027**:48–58.

Kastin AJ, Fasold MB, and Zadina JE (2002) Endomorphins, Met-enkephalin, Tyr-MIF-1, and the P-glycoprotein efflux system. *Drug Metab Dispos* **30**:231–234.

Kim SN, Seo JY, Jung W, Lee MY, Jung YS, and Kim YC (2007) Induction of hepatic CYP2E1 by a subtoxic dose of acetaminophen in rats: increase in dichloromethane metabolism and carboxyhemoglobin elevation. *Drug Metab Dispos* **35**:1754–1758.

Koba M and Konopa J (2005) [Actinomycin D and its mechanisms of action]. *Postepy Hig Med Dosw (Online)* **59**:290–298.

Kodama S and Negishi M (2006) Phenobarbital confers its diverse effects by activating the orphan nuclear receptor car. *Drug Metab Rev* **38**:75–87.

Labuz D, Mousa SA, Schäfer M, Stein C, and Machelska H (2007) Relative contribution of peripheral versus central opioid receptors to antinociception. *Brain Res* **1160**:30–38.

Lelong IH, Guzikowski AP, Haugland RP, Pastan I, Gottesman MM, and Willingham MC (1991) Fluorescent verapamil derivative for monitoring activity of the multidrug transporter. *Mol Pharmacol* **40**:490–494.

Letrent SP, Pollack GM, Brouwer KR, and Brouwer KL (1998) Effect of GF120918, a potent P-glycoprotein inhibitor, on morphine pharmacokinetics and pharmacodynamics in the rat. *Pharm Res* **15**:599–605.

Letrent SP, Pollack GM, Brouwer KR, and Brouwer KL (1999) Effects of a potent and specific P-glycoprotein inhibitor on the blood-brain barrier distribution and antinociceptive effect of morphine in the rat. *Drug Metab Dispos* **27**:827–834.

Lochhead JJ, McCaffrey G, Quigley CE, Finch J, DeMarco KM, Nametz N, and Davis TP (2010) Oxidative stress increases blood-brain barrier permeability and induces alterations in occludin during hypoxia-reoxygenation. *J Cereb Blood Flow Metab* **30**:1625–1636.

Lötsch J, Schmidt R, Vetter G, Schmidt H, Niederberger E, Geisslinger G, and Tegeder I (2002) Increased CNS uptake and enhanced antinociception of morphine-6-glucuronide in rats after inhibition of P-glycoprotein. *J Neurochem* **83**: 241–248.

Maund E, McDaid C, Rice S, Wright K, Jenkins B, and Woolacott N (2011) Paracetamol and selective and non-selective non-steroidal anti-inflammatory drugs for the reduction in morphine-related side-effects after major surgery: a systematic review. *Br J Anaesth* **106**:292–297.

McCaffrey G, Seelbach MJ, Staatz WD, Nametz N, Quigley C, Campos CR, Brooks TA, and Davis TP (2008) Occludin oligomeric assembly at tight junctions of the blood-brain barrier is disrupted by peripheral inflammatory hyperalgesia. *J Neurochem* **106**:2395–2409.

McGill MR, Williams CD, Xie Y, Ramachandran A, and Jaeschke H (2012) Acetaminophen-induced liver injury in rats and mice: comparison of protein adducts, mitochondrial dysfunction, and oxidative stress in the mechanism of toxicity. *Toxicol Appl Pharmacol* **264**:387–394.

Morgan MM, Fossum EN, Stalding BM, and King MM (2006) Morphine antinociceptive potency on chemical, mechanical, and thermal nociceptive tests in the rat. *J Pain* **7**:358–366.

Mutoh S, Osabe M, Inoue K, Moore R, Pedersen L, Perera L, Rebolloso Y, Sueyoshi T, and Negishi M (2009) Dephosphorylation of threonine 38 is required for nuclear translocation and activation of human xenobiotic receptor CAR (NR1I3). *J Biol Chem* **284**:34785–34792.

Pei JJ, Gong CX, An WL, Winblad B, Cowburn RF, Grundke-Iqbal I, and Iqbal K (2003) Okadaic-acid-induced inhibition of protein phosphatase 2A produces activation of mitogen-activated protein kinases ERK1/2, MEK1/2, and p70 S6, similar to that in Alzheimer's disease. *Am J Pathol* **163**:845–858.

Remy C, Marret E, and Bonnet F (2005) Effects of acetaminophen on morphine side-effects and consumption after major surgery: meta-analysis of randomized controlled trials. *Br J Anaesth* **94**:505–513.

Roberts LM, Black DS, Raman C, Woodford K, Zhou M, Haggerty JE, Yan AT, Cwirla SE, and Grindstaff KK (2008) Subcellular localization of transporters along the rat blood-brain barrier and blood-cerebral-spinal fluid barrier by in vivo biotinylation. *Neuroscience* **155**:423–438.

Romero-Calvo I, Ocón B, Martínez-Moya P, Suárez MD, Zarzuelo A, Martínez-Augustin O, and de Medina FS (2010) Reversible Ponceau staining as a loading control alternative to actin in Western blots. *Anal Biochem* **401**:318–320.

Ronaldson PT and Davis TP (2011) Targeting blood-brain barrier changes during inflammatory pain: an opportunity for optimizing CNS drug delivery. *Ther Deliv* **2**: 1015–1041.

Ronaldson PT and Davis TP (2013) Targeted drug delivery to treat pain and cerebral hypoxia. *Pharmacol Rev* **65**:291–314.

Ronaldson PT, Demarco KM, Sanchez-Covarrubias L, Solinsky CM, and Davis TP (2009) Transforming growth factor-beta signaling alters substrate permeability and tight junction protein expression at the blood-brain barrier during inflammatory pain. *J Cereb Blood Flow Metab* **29**:1084–1098.

Ronaldson PT, Finch JD, Demarco KM, Quigley CE, and Davis TP (2011) Inflammatory pain signals an increase in functional expression of organic anion transporting polypeptide 1a4 at the blood-brain barrier. *J Pharmacol Exp Ther* **336**:827–839.

Roninson IB, Chin JE, Choi KG, Gros P, Housman DE, Fojo A, Shen DW, Gottesman MM, and Pastan I (1986) Isolation of human mdr DNA sequences amplified in multidrug-resistant KB carcinoma cells. *Proc Natl Acad Sci USA* **83**:4538–4542.

Seelbach MJ, Brooks TA, Egleton RD, and Davis TP (2007) Peripheral inflammatory hyperalgesia modulates morphine delivery to the brain: a role for P-glycoprotein. *J Neurochem* **102**:1677–1690.

Shen KF and Crain AM (1997) Ultra-low doses of naltrexone or etorphine increase morphine's antinociceptive potency and attenuate tolerance/dependence in mice. *Brain Res* **757**: 176–190.

Simmons NL, Hunter J, and Jepson MA (1995) Targeted delivery of a substrate for P-glycoprotein to renal cysts in vitro. *Biochim Biophys Acta* **1237**:31–36.

Siddik SM, Aouad MT, Jalbout MI, Rizk LB, Kamar GH, and Baraka AS (2001) Diclofenac and/or propacetamol for postoperative pain management after cesarean delivery in patients receiving patient controlled analgesia morphine. *Reg Anesth Pain Med* **26**:310–315.

Takasato Y, Rapoport SI, and Smith QR (1984) An in situ brain perfusion technique to study cerebrovascular transport in the rat. *Am J Physiol* **247**:H484–H493.

Timsit YE and Negishi M (2007) CAR and PXR: the xenobiotic-sensing receptors. *Steroids* **72**:231–246.

Ueda K, Cardarelli C, Gottesman MM, and Pastan I (1987) Expression of a full-length cDNA for the human "MDR1" gene confers resistance to colchicine, doxorubicin, and vinblastine. *Proc Natl Acad Sci USA* **84**:3004–3008.

Van Aken H, Thys L, Veekman L, and Buerkle H (2004) Assessing analgesia in single and repeated administrations of propacetamol for postoperative pain: comparison with morphine after dental surgery. *Anesth Analg* **98**: 159–165.

Vanderah TW, Largent-Milnes T, Lai J, Porreca F, Houghten RA, Menzaghi F, Wisniewski K, Stalewski J, Sueiras-Diaz J, and Galyean R et al. (2008) Novel D-amino acid tetrapeptides produce potent antinociception by selectively acting at peripheral kappa-opioid receptors. *Eur J Pharmacol* **583**:62–72.

van der Marel CD, Peters JW, Bouwmeester NJ, Jacqz-Aigrain E, van den Anker JN, and Tibboel D (2007) Rectal acetaminophen does not reduce morphine consumption after major surgery in young infants. *Br J Anaesth* **98**:372–379.

Wang XQ, Sykes DB, and Miller DS (2010) Constitutive androstane receptor-mediated up-regulation of ATP-driven xenobiotic efflux transporters at the blood-brain barrier. *Mol Pharmacol* **78**:376–383.

Yousif S, Chaves C, Potin S, Margaill I, Scherrmann JM, and Declèves X (2012) Induction of P-glycoprotein and Bcrp at the rat blood-brain barrier following a subchronic morphine treatment is mediated through NMDA/COX-2 activation. *J Neurochem* **123**:491–503.

Zastre JA, Chan GN, Ronaldson PT, Ramaswamy M, Couraud PO, Romero IA, Weksler B, Bendayan M, and Bendayan R (2009) Up-regulation of P-glycoprotein by HIV protease inhibitors in a human brain microvessel endothelial cell line. *J Neurosci Res* **87**:1023–1036.

Zhang J, Huang W, Chua SS, Wei P, and Moore DD (2002) Modulation of acetaminophen-induced hepatotoxicity by the xenobiotic receptor CAR. *Science* **298**:422–424.

Address correspondence to: Lauren M. Slosky, Department of Pharmacology, College of Medicine, University of Arizona, 1501 N. Campbell Ave., P.O. Box 245050, Tucson, AZ 85724-5050. E-mail: lslosky@email.arizona.edu